Liquid Crystals
Publication details, including instructions for authors and subscription information:
http://www.informaworld.com/smpp/title~content=t713926090

Spectroscopic investigation of local molecular dynamics in liquid crystals I. Small molecules

L. Monnerie[a]; F. Laupretre[a]; C. Noel[a]
[a] Laboratoire de Physicochimie Structurale et Macromoléculaire, associé au CNRS, Ecole Supérieure de Physique et de Chimie Industrielles de la Ville de Paris, ParisCedex 05, France

To cite this Article Monnerie, L. , Laupretre, F. and Noel, C.(1988) 'Spectroscopic investigation of local molecular dynamics in liquid crystals I. Small molecules', Liquid Crystals, 3: 1, 1 — 29
To link to this Article: DOI: 10.1080/02678298808086346
URL: http://dx.doi.org/10.1080/02678298808086346

LIQUID CRYSTALS, 1988, VOL. 3, NO. 1, 1–29

Invited Article

Spectroscopic investigation of local molecular dynamics in liquid crystals

I. Small molecules

by L. MONNERIE, F. LAUPRETRE and C. NOEL
Laboratoire de Physicochimie Structurale et Macromoléculaire, associé au CNRS,
Ecole Supérieure de Physique et de Chimie Industrielles de la Ville de Paris,
10, rue Vauquelin, 75231 Paris Cedex 05, France

(*Received 3 August 1987*)

The dynamics of liquid crystal systems, consisting of either small molecules or polymer chains with main-chain or side-chain mesogenic groups, can be investigated using the same spectroscopic techniques which are applied to isotropic systems. This article briefly reviews ^{1}H, ^{13}C and ^{2}H N.M.R. and E.S.R. spectroscopy as well as dielectric relaxation. The particular features related to the oriented nature of the liquid crystal phases are developed. Typical examples of studies performed on small-molecule liquid crystals using these various spectroscopic techniques are described.

1. Introduction

The development of thermotropic liquid crystal polymers as either self-reinforced polymeric materials or materials for electronic displays and nonlinear optics requires a good knowledge of the local molecular motions in these polymers. Indeed, it is well known from the behaviour of ordinary polymers that mechanical or dielectric properties depend on the occurrence of transitions resulting from side-chain or main-chain motions. Although a complete understanding of the molecular dynamics of bulk polymers has not yet been achieved, spectroscopic investigations have led, in recent years, to a great improvement in the description of molecular motions in polymer systems. Thus, it is reasonable to expect that these results will play an important part in the analysis of local dynamics in liquid crystal polymers, even though very few experiments have yet been performed.

In this, the first article of a series, we review the type of information related to orientational order and dynamics that can be obtained by several spectroscopic techniques: ^{1}H, ^{13}C and ^{2}H N.M.R. and E.S.R. spectroscopy, as well as dielectric relaxation. Emphasis is given to the range of motional correlation times which can be investigated by each method. We also point out the specific treatment which is required for liquid crystal phases. Typical examples, chosen from studies performed on small-molecule liquid crystals, are discussed. In the second article, specific problems relating to the long-chain nature of liquid crystal polymers are examined. These include the difficulty in obtaining single-domain samples, easy supercooling leading to an ordered glass state and the occurrence of a glass–rubber transition, in

addition to the mesophase transitions. Results already obtained for these polymers by the above spectroscopic techniques are presented.

2. Structure and orientational behaviour of mesophases

2.1. *Structure of mesophases*

Thermotropic molecules can be organized in different ways, leading to characteristic structures for the mesophases. At high temperatures an isotropic liquid state is obtained, unless chemical degradation occurs. At lower temperatures various types of mesophases are observed, depending on the chemical structure of the compounds: a nematic phase (N) and different smectic phases (S). It is outside the scope of this article to describe the various structures; detailed descriptions can be found in [1, 2].

2.1.1. *Nematic*

In the ordinary nematic structure there is long-range orientational order of the molecular long axes. The average direction of these long axes defines the director **n** which may be treated as a vector, both directions of which ($+\mathbf{n}$ and $-\mathbf{n}$) are equivalent. In most cases the ordinary nematic structure shows optically positive uniaxial behaviour. It is worth noting that nematic liquid crystals possess a relatively low viscosity.

2.1.2. *Smectic A*

In smectic A phases the molecules are parallel to one another and are arranged in layers, with the molecular long axes perpendicular to the planes of the layers. Within each layer the lateral distribution of the molecules is random. The S_A phase exhibits optically positive uniaxial behaviour. Although the overall viscosity of smectic A phases is much higher than that of nematic phases, the molecules within the layers have a relatively high mobility.

2.1.3. *Smectic C*

The structure of the S_C phase is the tilted analogue of the S_A phase. Indeed, the molecules are arranged in layers, but with the molecular long axes tilted to the layer normal. The centres of gravity of the molecules are ordered randomly, and the molecules have a high mobility within the layers. The layers are free to slide over one another; that is, there is no long-range correlation, except of the tilt direction, between the layers. The S_C phases are optically biaxial.

2.1.4. *Smectic B*

In the S_B phase the molecules are arranged in layers, with the molecular long axes perpendicular to the planes of the layers, as in the S_A phase, but with the molecular centres in the layers positioned in a hexagonally close-packed array. There is long-range hexagonal order within the layers and some correlations between the layers. Nevertheless, the molecules are still able to rotate quite rapidly about their long axes; however, because of the hexagonal net dimension, the rotation has to be of a cooperative nature. In contrast to the phases previously described, which show a liquid-like behaviour, the S_B phase is structurally solid-like, though it exhibits shear and flow properties under stress.

2.1.5. *Smectic F*

In the S_F phase the molecules are packed in layers with their long axes tilted with respect to the layer planes; the tilt angle may be 20°. The molecular packing in the layers is hexagonal. Within the layers the correlation length is 20–30 molecules, but there is poor correlation between the layers.

2.1.6. *Temperature regimes of the various phases*

It has been observed that these phases appear in the following sequence when the temperature is decreased from that of the isotropic liquid:

$$I \rightarrow N \rightarrow S_A \rightarrow S_C \rightarrow S_F \rightarrow S_B.$$

All observed variants of the polymorphism can be derived from this sequence by cancelling one phase or several phases, depending on the chemical structure of the investigated compound.

2.2. *The orientational order parameter and the ordering potential*

2.2.1. *Nematic phases*

In nematic phases the average direction of orientation of the molecular long axes for the molecules defines the director **n**. The reference frame (x_4, y_4, z_4) associated with the mesophase is chosen so that the z_4 axis lies along the director **n**. If the liquid crystal molecules are taken to be rod-like, the degree of parallel order of the individual molecular long axis, z_2, is described by a single orientational order parameter:

$$\begin{aligned} S_{z_2z_4} &= \tfrac{1}{2}\langle 3\cos^2\beta - 1\rangle, \\ &= \bar{P}_2, \end{aligned}$$

where β is the angle between the individual molecular long axis and the director, the angular brackets indicate a thermal average and $P_2(\cos\beta)$ is the second Legendre polynomial.

In practice, liquid crystal molecules are not axially symmetric, but have an oblong structure leading to a blade-like shape in such a way that the two coordinate axes of the molecular frame normal to the long axis have different order parameters with respect to the director. The orientational order of the molecule must be described by a tensor with three principal values, $S_{x_2x_4}$, $S_{y_2y_4}$ and $S_{z_2z_4}$. As the tensor is traceless, the orientational order and its symmetry are completely described by only $S_{z_2z_4}$ and $\Delta = S_{x_2x_4} - S_{y_2y_4}$.

As a result of the long-range orientational correlation which characterizes the nematic phases, individual molecules are subject to an ordering potential U resulting from interactions with the surrounding molecules. In order to express this potential we have to consider the rotations from the molecular axis system (x_2, y_2, z_2) into the director axis system (x_4, y_4, z_4) defined by the Euler angles $\Omega = (\alpha, \beta, \gamma)$, defined in figure 1. For rod-like molecules, the general ordering potential has the form

$$U(\Omega) = \sum_{p=1}^{\infty} \gamma_{2p}\cos^{2p}\beta.$$

In practice, it appears that the highest-order terms ($p > 2$) are negligible, leading to

$$U(\Omega) = \gamma_2\cos^2\beta + \gamma_4\cos^4\beta.$$

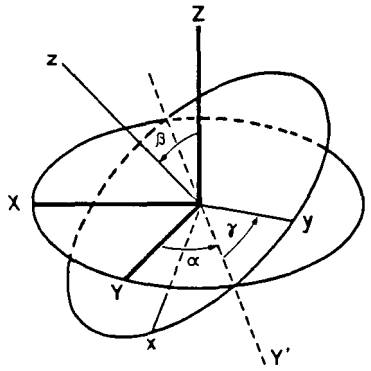

Figure 1. Rotational transformation of the original frame (X, Y, Z) to a new frame (x, y, z) through the Euler angles (α, β, γ).

Here β is the angle between the molecular z_2 axis and the director; the first term corresponds to the familiar Maier–Saupe potential [3]. For blade-like molecules, in which the molecular axes x_2 and y_2 have different alignments, a non-axially-symmetric ordering potential has to be considered:

$$U(\Omega) = \gamma_2 \cos^2\beta + \varepsilon \sin^2\beta \cos^2\alpha.$$

If z_2 is chosen as the molecular long axis which tends to align more closely with the director than either the x_2 or y_2 axis, then we have $|\gamma_2| > |\varepsilon|$; ε is proportional to the difference in the order parameters for the y_2 and x_2 axes, and $\varepsilon < 0$ corresponds to the y_2 axis being ordered preferentially to the x_2 axis along the director.

2.2.2. *Uniaxial smectic phases*

For smectic phases, in addition to the long-range orientational correlations there is some translational order due to the layer structure. However, for the spectroscopic techniques considered here only the orientational behaviour is of interest. For the uniaxial smectic phases S_A and S_B, the expressions for the order parameters and the restoring potential remain valid.

3. Spectroscopic methods for studying dynamics in liquid crystals

Most of the spectroscopic techniques used to study the dynamics of isotropic systems can be applied to the liquid crystal phases, in spite of the ordered structure. Depending on the mesophase, the molecular dynamics of these systems covers the range from the liquid state (motional frequency higher than 10^6 Hz) to the solid state. For this reason we shall describe different relaxation techniques which are applicable to the liquid and solid states. As previously stated, we will deal with ^1H, ^{13}C and ^2H N.M.R. and E.S.R. spectroscopy, as well as dielectric relaxation. It is worth noting that most of these spectroscopic techniques are used to investigate the orientational dynamics of specific groups of either liquid crystal molecules or extrinsic probes.

3.1. *General information obtainable by spectroscopic techniques*

In this section we review the type of information (e.g. order parameter or dynamics) that can be obtained by each technique, and indicate the motional frequency range which can be investigated using it. In each case references to specialist books or

review articles are given for the reader interested in detailed theoretical or technical information.

3.1.1. *^1H N.M.R.*

(For details see [4].) If we consider a pair of protons, with the H_1–H_2 internuclear vector, separated by a distance r, then measurement of the splitting $\Delta\nu$ between the two spectral lines as a result of dipolar coupling between the nuclear magnetic moments allows the orientational order parameter of the H_1–H_2 vector to be determined. The expression for $\Delta\nu$ is

$$\Delta\nu = \tfrac{1}{2}(3\gamma_H^2\hbar/2\pi r^3)\langle 3\cos^2\theta - 1\rangle,$$

where θ is the angle made by the H_1–H_2 vector with the external magnetic field, γ_H is the proton gyromagnetic ratio, and $\hbar$ is the Planck constant divided by 2π.

For real molecules, where the number of protons is generally more than two, the number of dipolar interactions is no longer unique and the spectrum becomes very complex. The measurement of the order parameters S in such systems by ^{1}H N.M.R. requires protons in some specific positions to be replaced by deuterons. For example, with the partially deuteriated 4-methoxy-benzylidene-4′-*n*-butylaniline (MBBA) molecule [5] the internuclear vector for the protons in positions ortho to each other is almost parallel to the molecular inertial axis (m), whereas the vector for the protons in positions meta to each other is almost perpendicular to m, and that for the protons in positions para to each other is at an angle of about 60°. Thus, ^{1}H N.M.R. allows the order parameters S for these different vectors to be determined, and the axially symmetric behaviour of the molecule to be tested.

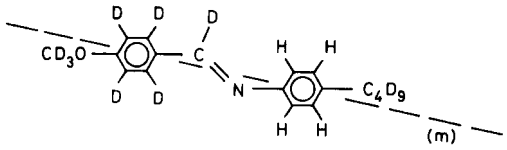

Detailed information on molecular dynamics is obtained mainly from the determination of the magnetic relaxation times T_1, $T_{1\varrho}$ and T_2. The magnetic relaxation in organic materials usually originates from modulation of dipolar proton–proton couplings, and therefore reflects the dynamics of the internuclear proton–proton vectors. For two protons separated by a distance r, the expression for the spin–lattice relaxation time T_1 and the spin–spin relaxation time T_2 are [4]

$$T_1^{-1} = (9/8)\gamma_H^4\hbar^2(J_1(\omega_H) + J_2(2\omega_H)),$$

$$T_2^{-1} = (9/32)\gamma_H^4\hbar^2(J_0(0) + 10J_1(\omega_H) + J_2(2\omega_H)),$$

where ω_H is the Larmor proton precession frequency. The spectral densities $J_m(m\omega)$ are Fourier transforms of the time correlation functions $F_m(\tau)$ of the second-order spherical harmonics:

$$J_m(\omega) = \int_{-\infty}^{\infty} \exp(-i\omega\tau)\langle F_m(0)\cdot F_m^*(\tau)\rangle\, d\tau.$$

The spectral densities involved in T_1 relaxation are taken at ω_H and $2\omega_H$. Therefore, in order to make an effective contribution to T_1, the molecular motions have to possess

a frequency near the Larmor proton frequency. This, depending on the applied magnetic field, corresponds to motional correlation times in the range 2×10^{-12} to 10^{-5} s. From the expression for T_2 it can be seen that T_2 values are affected by the same molecular motions as T_1, but also by the low-frequency motions. It should be recalled that T_2 is inversely proportional to the linewidth for liquid-like compounds. The longitudinal relaxation time in the rotating frame, $T_{1\varrho}$, depends on the spectral densities at frequencies ω_1 and $2\omega_1$, where ω_1 is the strength of the applied r.f. field expressed in angular frequency units. Consequently, $T_{1\varrho}$ will be sensitive to motions with correlation times in the range 10^{-4} to 10^{-6} s, depending on the strength of the applied r.f. field.

As a result of r^{-6} dependence of the dipolar interactions, most of the intramolecular contributions to relaxation measured from ^{1}H N.M.R. will correspond to two protons bonded to the same carbon atom, or to two adjacent carbon atoms. However, when using ^{1}H N.M.R. to study the dynamics of molecules in a condensed phase, in addition to the intramolecular reorientation contribution to the relaxation processes there is a contribution from intermolecular ^{1}H–^{1}H interactions. These interactions are related to self-diffusional translation motions of molecules, changing the ^{1}H–^{1}H intermolecular distance. The molecular description is based on molecular translation diffusion coefficient D and the distance d of closest approach between the protons of neighbouring molecules. It has to be pointed out that the intra- and intermolecular contributions can be separated by measuring T_1 or $T_{1\varrho}$ for protonated molecules at various concentrations in perdeuteriated solvents [6]. Such solutions may be solids or liquids.

3.1.2. *^{13}C N.M.R.*

(For more detailed information see [4, 7–9].) ^{13}C occurs naturally in the skeleton of molecules, but in low isotopic abundance ($\sim 1\%$), so there is no dipolar coupling between ^{13}C spins. However, there is still dipolar coupling with proton spins. The main advantage of ^{13}C N.M.R. is that in the liquid state the resonance lines of the different carbon atoms of a molecule are usually sufficiently well separated to allow the individual molecular sites to be differentiated. If a purely ^{13}C–^{1}H dipolar relaxation mechanism is assumed, the spin–lattice relaxation time T_1 obtained from a ^{13}C experiment is given by

$$T_1^{-1} = (3/48)\gamma_C^2\gamma_H^2\hbar^2[J_0(\omega_H - \omega_C) + 18J_1(\omega_C) + 9J_2(\omega_H + \omega_C)].$$

The spectral densities J are inversely proportional to the sixth power of the ^{13}C–^{1}H distance, and consequently only directly bonded protons contribute to the ^{13}C relaxation of protonated carbons. In particular, intermolecular contributions are negligible, in contrast to ^{1}H relaxation. From this expression for T_1^{-1} it is clear that in the liquid state molecular motions in the range 5×10^{-12} to 10^{-8} s are effective in T_1 relaxation.

For lower-frequency motions in either liquids or solids, $T_{1\varrho}$ measurements, corresponding to spin–lattice relaxation in the rotating frame, reflect motions with correlation times from 10^{-4} to 10^{-6} s.

In a similar way, useful information can also be obtained from the chemical shift anisotropy of the ^{13}C spectral lines. Indeed, the lineshape depends on the averaging of the chemical shift anisotropy tensor by the molecular motions; however, to obtain a significant effect correlation times shorter than 10^{-4} s are required. Measurements of the chemical shift anisotropy can yield the orientational order parameter S of the molecular long axis [10].

From these considerations it is clear that ^{13}C N.M.R. provides a very powerful means of investigating molecular dynamics. In addition to measurements on liquid systems, it can now be applied to solid samples, using high-resolution solid-state N.M.R. spectrometers.

3.1.3. *^2H N.M.R.*

(For detailed information see [9, 11, 12].) Deuterium, ^2H, is a nucleus particularly suited to the study of orientation and polymer dynamics. Deuterons represent well-defined nuclear spin labels with spin I of 1, the N.M.R. parameters of which are almost exclusively governed by the quadrupolar interaction with the electric field gradient tensor (FGT) at the deuteron site. Although the intermolecular contributions to the electric field gradient can be significant [13], the field gradient usually originates mainly from the electrons in the C–^2H bond and is considered to a first approximation to be intramolecular. It is found to be axially symmetric about the C–^2H bond in aliphatic compounds, and also (to a good approximation) in aromatic compounds as well. Thus, information obtained by ^2H N.M.R. on molecular order and dynamics concerns individual C–^2H bond directions.

As deuterium has spin $I = 1$, the N.M.R. spectrum in the absence of motion is a typical quadrupolar doublet, with a symmetric splitting $\Delta\nu$. In the solid state, $\Delta\nu$ is given by

$$\Delta\nu = \frac{e^2qQ}{4\hbar}(3\cos^2\theta - 1 - \eta\sin^2\theta\cos^2\phi),$$

where $e^2qQ/\hbar$ is the quadrupolar coupling constant, η is the asymmetry parameter, and the orientation of the magnetic field in the principal axis system of the FGT is specified by the polar angles θ and ϕ. In the simplest case, with $\eta \approx 0$, θ is then the angle between the C–^2H bond direction and the external magnetic field. The magnitude of $\Delta\nu$ is then directly related to the orientation of the C–^2H bonds in the sample relative to the magnetic field; it can be used therefore to determine the order parameter of rigid, ordered systems. Moreover, for mobile ordered systems, where there is a rapid uniaxial motion of the C–^2H bond around the long molecular axis, the value of the splitting yields the order parameter corresponding to the C–^2H bond. As the ^2H N.M.R. spectrum is usually well resolved, this is a means of measuring the order parameters S of various C–^2H bonds, and thus of getting information about the conformational states of the different C–^2H groups in the molecule in the mesomorphic state.

^2H N.M.R. is also a very powerful means of studying of molecular dynamics since it covers a frequency range from 10^{-1} to 10^{10} Hz. Standard measurements of the spin–lattice relaxation time T_1, which involves spectral densities at ω_{2H} and $2\omega_{2H}$, ω_{2H} being the Larmor frequency for deuterium, yield information in the N.M.R. frequency (10^8–10^{10} Hz), whereas various methods such as lineshape analysis, solid echo and spin alignment allow the characteristics of the motion to be determined in the frequency ranges 10^7–10^8 Hz, 10^5–10^8 Hz, 10^4–10^{-1} Hz, respectively. Furthermore, it is worth noting that for motions with frequencies below 10^8 Hz, ^2H N.M.R. can also discriminate between the different types of reorientation mechanisms, for example, libration, jumps or rotational diffusion. For the purpose of testing models of molecular motion, an interesting pulse sequence has recently been developed [14] which allows the individual spectral densities for the various magnetic relaxation times to be determined.

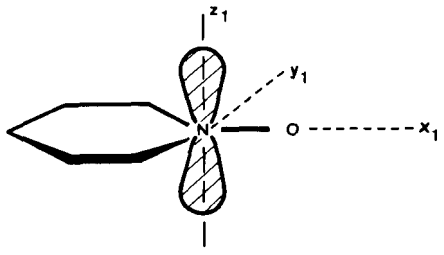

Figure 2. Principal magnetic axes of a nitroxide radical, and representation of the 2p π atomic orbital of the nitrogen atom.

Table 1. Designations and formulae of nitroxide probes.

Designation	Formula
Tempol	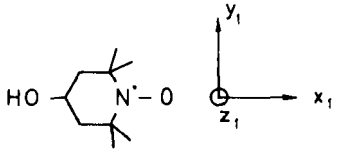
P.D. Tempone	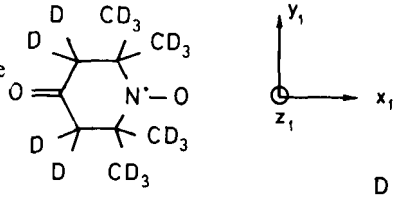
P-Probe	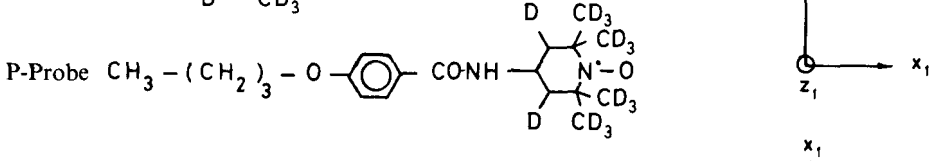
CSL	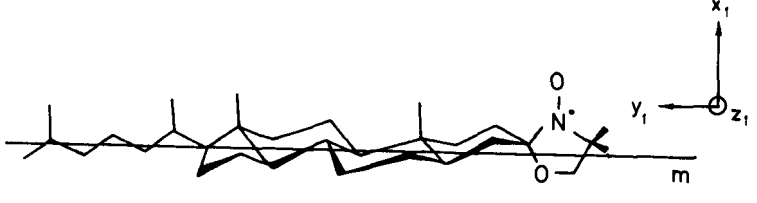

3.1.4. *E.S.R.*

(For detailed information see [15–18].) In contrast to ^{1}H, ^{2}H and ^{13}C N.M.R., the study of molecular dynamics by E.S.R. requires the use of a free-radical probe. In most cases a nitroxide group is used because of its high stability, but biradical spin probes have also been used [19]. The various nitroxide probes considered here are listed in table 1. In nitroxide radicals, the odd electron is largely confined to a 2p π atomic orbital in the nitrogen atom. This is shown in figure 2, together with the magnetic axes which diagonalize the **g**-tensor and the hyperfine tensor, **A**. The hyperfine coupling of the free electron with the $I = 1$ nuclear spin of nitrogen leads to three transitions and an E.S.R. spectrum with three lines. The hyperfine coupling depends on the orientation of the magnetic axes relative to the applied magnetic field.

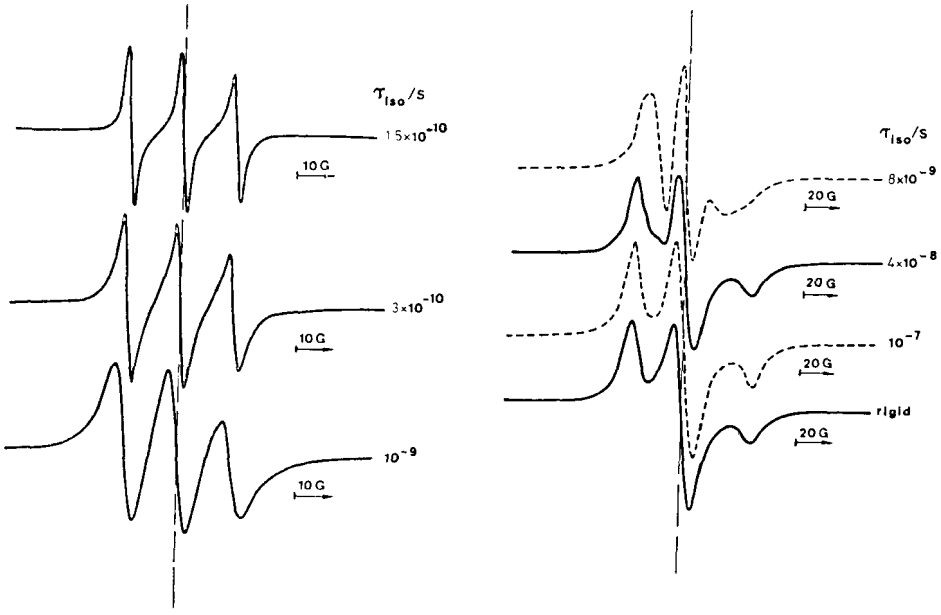

Figure 3. Typical E.S.R. spectra of a nitroxide probe in an isotropic medium. The corresponding correlation times τ_{iso} of the isotropic motion of the probe are indicated.

If the nitroxide group undergoes a motion, the hyperfine coupling will be modulated. However, because of the rather large value of this coupling only motions with correlation times τ shorter than 10^{-8} s can have a significant averaging effect.

As in N.M.R. experiments, relaxation times T_1 and T_2 can be determined. In practice the dynamical properties of a spin probe are reflected in the linewidths, which are inversely proportional to the transverse relaxation time T_2. For nitroxide radicals, the dominant contributions to T_2 are the motional modulations of the hyperfine and **g**-tensor interactions. The corresponding spectral densities involve both low- and high-frequency motions. As shown in figure 3, in unoriented samples the E.S.R. spectra can have very different appearances, depending on the mobility of the nitroxide group. At high mobility ($\tau < 10^{-9}$ s) a well-resolved spectrum with three lines is observed, whereas for a powder sample, in which the nitroxide molecules may have any orientation, an almost structureless spectrum is recorded. For intermediate mobilities the linewidth of each line can be measured and the corresponding correlation time derived. For correlation times 10^{-9} s $< \tau < 5 \times 10^{-8}$ s, the spectrum has to be simulated in order to obtain τ. A computer program for this is given in Chapter 3 of [15].

In oriented samples, the E.S.R. spectrum depends on the orientation of the nitroxide group with the applied magnetic field, so it is possible therefore to measure the group's orientational order parameter S. Thus, for a single-domain liquid crystal sample, an E.S.R. spectrum recorded with the magnetic field parallel (or perpendicular) to the director allows the order parameters of the nitroxide magnetic axes relative to the applied magnetic field to be determined (see Chapter 10 of [15]). If the nitroxide group is covalently bound to another chemical group in the probe molecule, the order parameter of a given molecular axis of the probe can be deduced from the measured order parameter if the angle between the two axes is known. It should be

noted that the order parameter which is determined is for the nitroxide molecules in the liquid crystal, not the liquid crystal molecules themselves. This is an important point (which will be illustrated later) because, depending on the chemical structure and the shape of the nitroxide molecule, the probe can be located either close to the rigid core of the liquid crystal molecules or in the region of the flexible tails.

3.1.5. *Dielectric relaxation*

(For details see [20–24].) Molecules with a permanent electric dipole moment respond to an electrical field in such a way that when an external field is applied, the interaction between the field and the dipole moment changes the probability distribution of the molecular orientation. For nematic phases [25, 26] the static permittivities ($\varepsilon_{\parallel}^{0}$ and $\varepsilon_{\perp}^{0}$) and the high-frequency permittivities ($\varepsilon_{\parallel}^{\infty}$, $\varepsilon_{\perp}^{\infty}$) corresponding to the electric field parallel or perpendicular to the director depend on the orientational order parameter S, the longitudinal and transverse components of the molecular dipole moment and the molecular polarizability tensor, the lengths of the long and short axes of the molecular ellipsoid, and two quantities $g_{\parallel}$ and $g_{\perp}$ that describe the molecular dipole correlations parallel or perpendicular to the director. Although the dielectric anisotropy $\Delta\varepsilon = \varepsilon_{\parallel} - \varepsilon_{\perp}$ is a function of the order parameter, S cannot be derived from measurements of $\Delta\varepsilon$. However, if S is determined by another technique and the relevant molecular quantities are known, then $g_{\parallel}$ and $g_{\perp}$ can be obtained from $\Delta\varepsilon$.

Information on the dynamic behaviour of dipolar groups is provided by the frequency dependence of the complex dielectric permittivity, $\varepsilon^{*}(\omega)$. The real and imaginary parts of the complex permittivity are usually denoted by $\varepsilon'(\omega)$ and $\varepsilon''(\omega)$, respectively; $\varepsilon'(\omega)$ corresponds to the in-phase response and is associated with the recoverable energy, whereas $\varepsilon''(\omega)$ is the quadrature response related to the energy dissipated by dipole motions. The quantity $\varepsilon^{*}(\omega)$ can be expressed using the time–frequency Fourier transform relation involving the time correlation function of the instantaneous macroscopic dipole moment $\mathbf{M}$:

$$p(\omega)(\varepsilon^{*}(\omega) - \varepsilon^{\infty})/(\varepsilon^{0} - \varepsilon^{\infty}) = 1 - i\omega \int_{0}^{\infty} \phi(t) \exp(-i\omega t)\, dt,$$

$$\phi(t) = \langle \mathbf{M}(0) \cdot \mathbf{M}(t) \rangle / \langle \mathbf{M}(0) \cdot \mathbf{M}(0) \rangle,$$

where $p(\omega)$ is an internal field correction which is close to unity; $\mathbf{M}$ represents the vector sum of the elementary dipole moments, and thus the quantities $\langle \mathbf{M}(0) \cdot \mathbf{M}(t) \rangle$ and $\langle \mathbf{M}(0) \cdot \mathbf{M}(0) \rangle$ contain both the autocorrelation and cross-correlation functions associated with the elementary dipole moments. For isotropic systems of small molecules, each of them with a dipole moment $\boldsymbol{\mu}$, the cross-correlation terms describing the correlation of motions of different molecules is generally ignored, and only the orientational autocorrelation function is considered:

$$\phi(t) = \langle \boldsymbol{\mu}(0) \cdot \boldsymbol{\mu}(t) \rangle / \mu^{2}.$$

In isotropic systems of polymer chains with dipolar units, there is an angular correlation between the dipolar groups along each chain. However, it has been shown [27] that the time dependence of any cross-correlation term is the same as that of the autocorrelation term of a unit in the chain.

It is worth noting that dielectric relaxation involves the first-order spherical harmonic, unlike the N.M.R. and E.S.R. relaxation times, which are related to the second-order spherical harmonics.

For the ordered phases of small-molecule liquid crystals, dielectric relaxation experiments can be performed on single-domain samples with the electric field oriented either parallel or perpendicular to the director. The relevant quantities are the parallel or perpendicular component of the dipole moment, $\mu_\parallel$ or $\mu_\perp$, which are functions of the longitudinal and transverse components of the dipole moment for the ellipsoidal molecules.

There is great interest in dielectric relaxation because of the wide frequency range which can be investigated, and the fact that the frequency-dependent permittivity may be inverted to give the time-dependent correlation function over a large time domain. By contrast, N.M.R. and E.S.R. only yield certain Fourier components of the time-dependent correlation function. In practice, the high-frequency range is limited by the available equipment to 30×10^9 Hz; in the low-frequency range conductivity processes are frequently superimposed on the relaxation behaviour below 10^4 Hz, but they can be subtracted since their frequency dependence is well known. Thus, for liquids it is possible to obtain dynamical information down to 1 Hz. For solids, for which the conductivity contribution is very low, information on motion can be obtained down to 10^{-4} Hz. Consequently a very broad frequency range is covered, without any gap.

Finally, it is worth noting that when several dipolar groups are present in a molecule, even if separate dielectric relaxations are observed, there is no direct way of assigning a given relaxation to a specific polar group. This has to be done by comparison with results obtained by other techniques, or by studying a set of molecules whose chemical structure is gradually changed.

3.2. *Characteristic features of spectroscopic studies of dynamics in liquid crystals*

In all the spectroscopic techniques considered here, the motion of the molecules under investigation is measured through tensorial quantities, the values of which are changed by rotation of the molecule relative to the fixed laboratory frame. Thus, on going from the coordinate system associated with the investigated quantity (e.g. dipole moment, internuclear vector, or magnetic axes) to the laboratory frame, we have to consider several intermediate systems. The transformations from one system to another are defined by sets of Euler angles (figure 1). These reference systems are passed through in the following order:

(1) The principal axis system, $F_1(x_1, y_1, z_1)$ associated with the particular molecular quantities.
(2) The diffusional axis system of the molecule, F_2, which corresponds to the principal axes of the molecular rotational diffusion tensor (this tensor is well defined for a rigid molecule of high symmetry; although the definition is more questionable for flexible molecules, it is useful in molecular dynamics). Usually it is assumed that the principal molecular axes for the ordering tensor are the same as for the rotational diffusion tensor. The transformation from F_1 to F_2 is defined by Euler angles $\Theta_1 = (\alpha_1, \beta_1, \gamma_1)$.
(3) The instantaneous director system, F_3, which characterizes the orientational state, at a given time, of the surroundings of the molecule considered. The transformation $F_2 \rightarrow F_3$ is described by the Euler angles Θ_2.
(4) The average director system, F_4, of a domain (or of the sample if it is a single-domain sample). Usually this system is chosen so that the director lies along z_4. F_3 and F_4 are related through the Euler angles Θ_3.

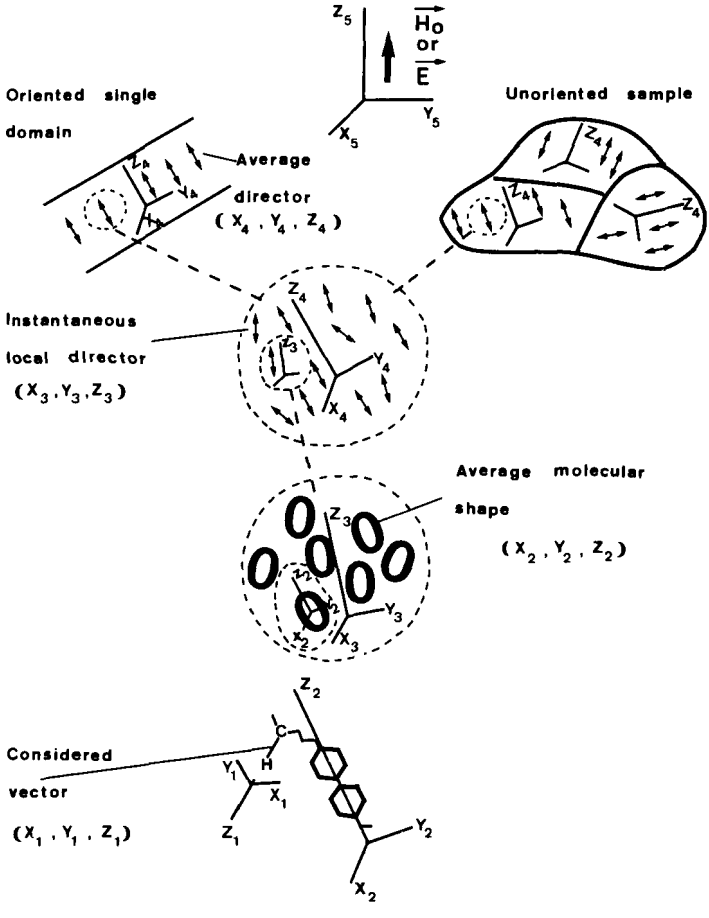

Figure 4. Schematic diagrams of the different frames considered in liquid crystals.

(5) The laboratory system, F_5. The transformation from F_4 to F_5 corresponds to the angles Θ_4.

These frames are shown schematically in figure 4.

The coordinate transformations Θ_i ($i = 1, 2, 3, 4$) allow us to incorporate the time-scales and amplitudes of the various physical motions which are implied in the dynamics of liquid crystal phases and affect the measurements performed in the laboratory frame. This procedure has been applied for each spectroscopic technique; the complete developments are given for N.M.R. and E.S.R. in [28, 29] and for dielectric relaxation in [30]. Here we shall focus on the particular types of motion in each transformation.

3.2.1. *$F_1 \rightarrow F_2$ (principal axes to diffusional system)*

Since liquid crystal molecules usually have some internal flexibility, the rotational diffusion axes correspond to the diffusion behaviour averaged over the various conformations of the molecules. The transformation $F_1 \rightarrow F_2$ describes the intramolecular motions performed by the molecular group observed by the particular

spectroscopic technique. For example, in the molecule

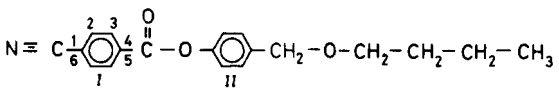

the ^{13}C N.M.R. T_1 or $T_{1\varrho}$ values for the carbon atoms 2, 3, 5 and 6 will be affected by the rotation of the phenyl ring I about its C_1-C_4 axis. Similarly, the rotation of the terminal CH_3 group around the CH_2-CH_3 bond or the trans–gauche conformational changes of the CH_2 groups may contribute to the relaxation of carbon atoms in the chain (a detailed discussion is given in [31]). In dielectric measurements, the motion of the nitrile electric dipole will characterize the intramolecular motion of the C_1-C_4 axis of the phenyl ring I, whereas the CH_2-O-CH_2 dipole will be related to the intramolecular motions associated with both the tail and the phenyl ring II.

In E.S.R., the nitroxide group, the orientational motion of which is observed, may in some probe molecules (table 1) have imparted to it an intramolecular motion, as for example in the P-probe. However, in the CSL probe the nitroxide group is rigidly fixed in the molecule, although the principal magnetic axes involved in the relaxation do not coincide with the rotational diffusion frame.

It has to be pointed out that all these intramolecular motions often occur in a high frequency range (10^9–10^{11} Hz).

3.2.2. $F_2 \rightarrow F_3$ *(diffusional system to instantaneous director)*

This transformation corresponds to the rotational diffusion motion of a liquid crystal molecule relative to the surrounding oriented molecules. By considering the intramolecular motions of the various constituent groups, a mean shape may be assigned to the molecule as a whole: either a rod or a blade. The complete description of the diffusion of a rigid blade requires three diffusion constants corresponding to rotational motion around the molecular long axis and the two different perpendicular axes. However, as the values of these last two diffusion constants are very similar, the diffusional motion is usually treated as for a rigid rod molecule. The characteristic diffusion coefficients are then $D_\parallel$ for motion about the molecular long axis, and $D_\perp$ for motion about the perpendicular axis; the corresponding correlation times are $\tau_{R\parallel}$ and $\tau_{R\perp}$ respectively ($\tau_{R\perp} = 1/6D_\perp$). The extent of anisotropy is described by the anisotropy coefficient $N = D_\parallel/D_\perp$. The coefficients $D_\parallel$ and $D_\perp$ are sometimes difficult to determine accurately, and often only a mean diffusion coefficient $\bar{D} = (D_\parallel D_\perp)^{1/2}$ and a mean correlation time $\bar{\tau}_R = (\tau_{R\parallel}\tau_{R\perp})^{1/2}$ are obtained.

In many cases, instead of considering the asymmetric shape of the molecule and the resulting anisotropic motion, the molecule is treated as a sphere, and its rotational diffusion behaviour is treated as an isotropic motion characterized by a single diffusion coefficient, D_{iso}, and a single correlation time, τ_{iso}. Of course, such a crude approximation makes the analysis much simpler.

We now consider the motional models used to describe the rotational diffusion process of the molecule, independently of its shape. Several models have been developed for various frequency ranges and sizes of molecule. For fast motion, i.e. $\tau < 10^{-9}$ s, a brownian rotational diffusion is always considered; this corresponds to an infinitesimal reorientation of the molecule following each collision with the surrounding molecules. For slower motion, in addition to this brownian model (which seems to account fairly well for the motion of bulky molecules) two other models have been proposed. The first one is the jump diffusion model, in which the molecule has

a fixed orientation for a time τ and then jumps instantaneously to a new orientation; the second one is the free-diffusion model, in which the molecule rotates freely by its momentum for a time τ, and then reorients itself instantaneously in a new direction. These two models have been applied satisfactorily to small molecules, the motions of which are slowed by the high viscosity of the surrounding medium. Another model often encountered in the description of molecular dynamics in liquid crystals is the strong collision model, which assumes that the molecular orientations before and after a collision are quite uncorrelated [32].

These features concern molecular motion in both isotropic media and ordered systems, such as liquid crystal phases. The situation is different when dealing with the type of restoring potential applied to the mobile molecule. Indeed, for ordinary liquids or polymers an isotropic potential is considered, while for liquid crystal phases we have to use either an axially symmetric potential (assuming a rod-like molecule) or a non-axially-symmetric potential (assuming a blade-like molecule). The expressions for these ordering potentials are given in §2.2. E.S.R. data have been analysed by using such expressions [33, 34].

It should be noted that the thermal averages of these fast molecular motions give the orientational order parameters, **S**. Thus the spectroscopic techniques applied to dynamical studies will also yield the order parameters.

3.2.3. *$F_3 \rightarrow F_4$ (instantaneous director to average director)*

So far we have discussed diffusional molecular motion relative to the local environment, which in liquid crystals has a temporary order, leading to an instantaneous director. With time, this instantaneous local director undergoes orientational changes relative to the average director, which is the same as the director of the domain. The transformation $F_3 \rightarrow F_4$ accounts for these fluctuations of the instantaneous local director.

One mechanism for these fluctuations lies in orientational order director fluctuations (O.D.F.s), which are collective elastic fluctuations in the deformations of liquid crystals resulting from hydrodynamic effects [35, 36]. These fluctuations can be analysed in relaxation modes with a wave-vector **q** corresponding to dimensions much greater than the molecular size. If we describe the distortion behaviour of the liquid crystal phase using a single elastic constant K (an average of the three elastic constants K_1, K_2 and K_3) and an average viscosity η, the amplitude of the mode q waves is proportional to kT/Kq (where T is the absolute temperature), and the relaxation time τ_q, which characterizes the highly damped viscous relaxation of the waves, is given by $\tau_q^{-1} = Kq^2/\eta$. A typical value for the fastest mode is $\sim 10^{-8}$ s, but the amplitude of these waves is very small, making them of low efficiency for dynamic measurements in this time range. This means that O.D.F.s will not affect E.S.R. lineshapes or relaxation times T_1 measured in high magnetic field N.M.R. experiments. On the other hand O.D.F.s will contribute to relaxation times T_1 measured in low magnetic field N.M.R. experiments, as well as to relaxation times $T_{1\varrho}$ and to dielectric relaxation studies at frequencies lower than 10^7 Hz. In the frequency range where O.D.F. mechanism makes a significant contribution, T_1 is expected to show a $\omega^{-1/2}$ frequency dependence, characteristic of O.D.F.s. Furthermore, T_1^{-1} is proportional to $T\eta^{1/2}/K^{3/2}$.

Another mechanism, called the slowly relaxing local structure (S.R.L.S.), has been proposed to account for the orientational changes of the local director [34]. In contrast to the O.D.F. mechanism, which operates on a scale much larger than the molecular size, the S.R.L.S. model deals with processes at a molecular level. The

motion of one molecule (such as those described here) is considered to take place inside a cage consisting of neighbouring molecules, but because of the constraints arising from the cage the correlation function does not go to zero. As a result of the translational and rotational diffusion of the constituent molecules the cage structure slowly changes, leading to a complete averaging of the orientation of the molecule considered. A crude estimate of the relaxation time of this cage structure leads to values in the range 10^{-9} s to 3×10^{-8} s. The S.R.L.S. mechanism can contribute efficiently to the high frequency spectroscopic measurements.

3.2.4. *$F_4 \rightarrow F_5$ (average director to laboratory frame)*

In single-domain liquid crystal samples, the transformation from the average director system to the laboratory frame is well defined. In many experiments the sample is oriented in such a way that the director lies along the magnetic field. However, useful complementary information can be obtained by changing the orientation of the director relative to the magnetic field.

In multi-domain samples, the domains have different orientations such that on the scale of a single domain there is local ordering, but the whole sample appears macroscopically disordered. In order to make the transformation $F_4 \rightarrow F_5$ the distribution of the domain directors has to be known. As this distribution is frequently unknown, the investigation of multi-domain samples is considerably more difficult than that of a single domain. Unfortunately there is sometimes no alternative, even with small-molecule liquid crystals (as for example in some smectic phases).

4. Examples of dynamic behaviour in small-molecule liquid crystals

Applications of the various spectroscopic techniques to the investigation of molecular dynamics in liquid crystal phases will be illustrated for small molecules. As many studies have been performed on such systems, we shall consider the most typical. The structures of the various molecules are given in table 2.

Table 2. Designations and formulae of liquid crystal molecules discussed.

Designation	Formula
MBBA	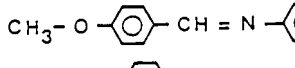
TBBA	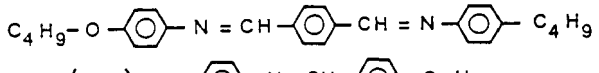
40–6	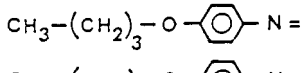
50–6	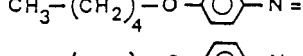
50–7	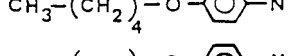
50–8	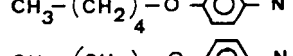
60–6	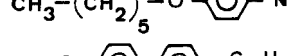
5CB	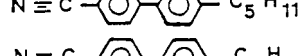
7CB	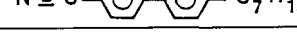

4.1. ^1H N.M.R.

Intra- and intermolecular motions contribute to the relaxation processes in ^1H N.M.R. This leads to a more complex analysis, but when enough data are available ^1H N.M.R. relaxation is a particularly useful means of studying intermolecular motions. Measurements of T_1 have been made on MBBA in the nematic phase from 18 to 45°C [37] over a very broad frequency range (2 kHz–270 MHz) using the field cycling technique in the low-frequency domain. The dependence of T_1 on the angle between the magnetic field and the director is consistent with the O.D.F. mechanism being the only relaxation process. Indeed, no angular dependence is expected for the self-diffusion (S.D.) mechanism. The frequency dependence of T_1 can be analysed by considering three contributions: O.D.F., S.D. and reorientational (R) motions of the molecule. Assuming that there are no cross-terms, the expression

$$T_1^{-1} = P_{ODF} T_{1ODF}^{-1} + P_{SD} T_{1SD}^{-1} + P_R T_{1R}^{-1},$$

is obtained, where P_i represents the fraction of the 21 protons per molecule associated with the ith mechanism. Therefore, since the high flexibility of the MBBA side-chains means that the O.D.F. mechanism is most probably restricted to the nearest neighbours

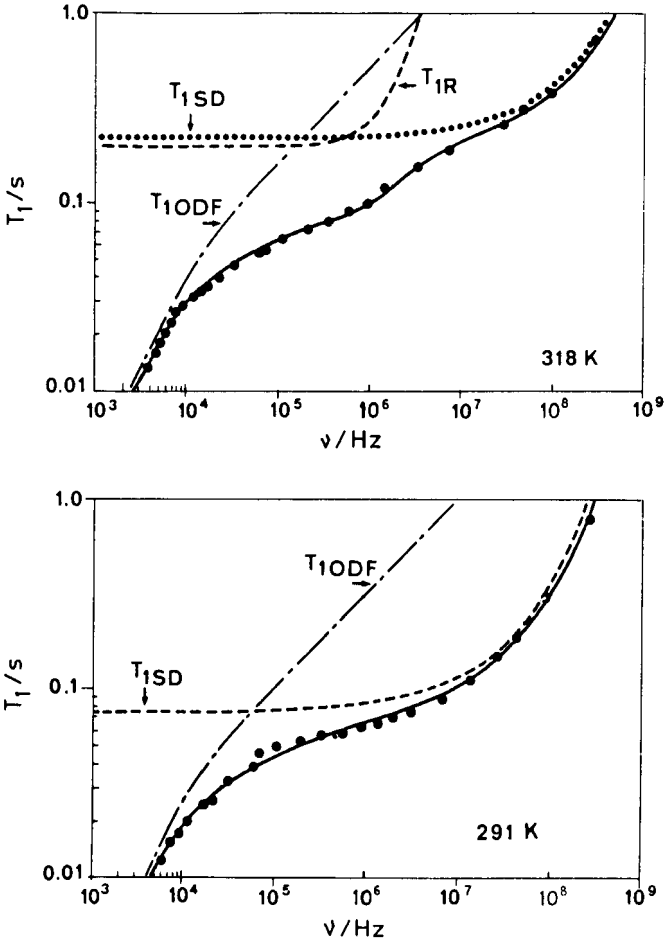

Figure 5. T_1 proton–spin relaxation dispersion and T_{1ODF}, T_{1SD} and T_{1R} contributions for MBBA at 318 and 291 K. (After [37].)

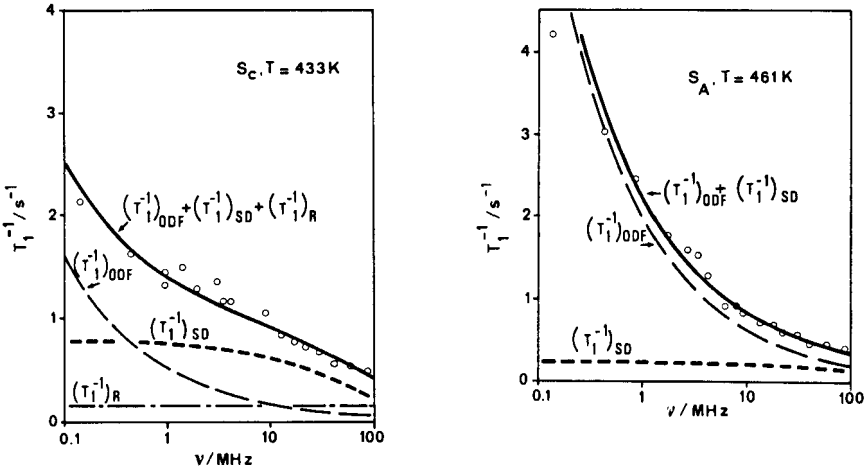

Figure 6. T_1 proton–spin relaxation dispersion in the S_C and S_A phases of TBBA. (After [38].)

Table 3. Characteristic parameters in the self-diffusion and rotation model of nematic MBBA, from ^{1}H N.M.R. [37].

T/K	τ(SD)/s	D(SD)/cm^2 s^{-1}	d/Å	τ_R/s
291	$1{\cdot}21 \times 10^{-9}$	$0{\cdot}98 \times 10^{-7}$	2·67	$2{\cdot}43 \times 10^{-7}$
300	$0{\cdot}65 \times 10^{-9}$	$1{\cdot}78 \times 10^{-7}$	2·64	$1{\cdot}45 \times 10^{-7}$
308	$0{\cdot}50 \times 10^{-9}$	$2{\cdot}27 \times 10^{-7}$	2·61	$0{\cdot}94 \times 10^{-7}$
318	$0{\cdot}30 \times 10^{-9}$	$3{\cdot}47 \times 10^{-7}$	2·50	$0{\cdot}57 \times 10^{-7}$

of the eight ring protons, $P_{ODF} = 8/21$. All the protons participate to the S.D. process, so $P_{SD} = 1$. Rotational motion about the long molecular axis is very rapid and does not contribute to the rotation mechanism (neither do the CH_2 or CH_3 intramolecular motions), and thus rotation about the perpendicular axis is the only one that does participate. The fit of the experimental curves to such an analysis leads to the results shown in figure 5, and to the values of the molecular quantities of interest reported in table 3. The activation energy associated with the self-diffusion process, $E_{SD} = 37\,\text{kJ mol}^{-1}$, and the very small pre-exponential factor, $D_0 = 0{\cdot}34\,\text{cm}^2\,\text{s}^{-1}$, suggest some kind of cooperative diffusional motion. At high temperatures only rotation about the perpendicular axis contributes to the spin relaxation. O.D.F. is the dominant relaxation mechanism at low frequencies, up to about 10^5 Hz, as would be expected from the hydrodynamic fluctuations involved.

Similar studies have been carried out on terephthalylidene-bis-(4-*n*-butyl-aniline) (TBBA) (see table 2) in its S_A and S_C phases [38], and the resulting curves are shown in figure 6. It appears that there is a higher contribution from the S.D. mechanism in the S_C than in the S_A phase, and the rotation of the molecule about the perpendicular axis contributes to the relaxation in S_C, whereas it does not in S_A. In the S_A phase T_1 is dominated by the O.D.F. mechanism.

The isotopic dilution method, used to separate the inter- and intramolecular contributions (mainly S.D. and O.D.F., respectively) has been applied to T_1 and $T_{1\varrho}$ on 4-*n*-pentyl-4′-cyanobiphenyl (5CB) [39]; the results are shown in figure 7.

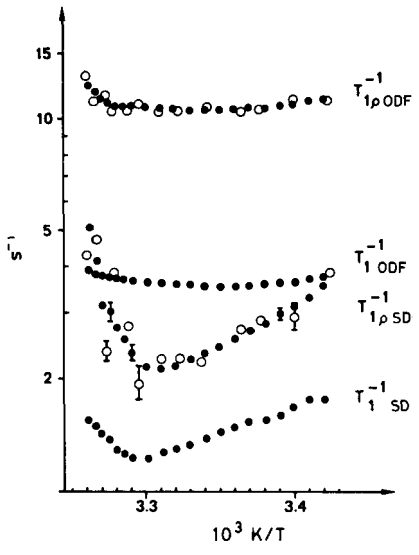

Figure 7. Intermolecular (S.D.) and intramolecular (O.D.F.) contributions to the T_1 and $T_{1\varrho}$ relaxation times plotted against $10^3/T$ for 5CB. (After [39].)

4.2. ^{13}C *N.M.R.*

In spite of the various advantages of using ^{13}C N.M.R. to investigate molecular dynamics, it has only been used in a limited number of such studies on small-molecule liquid crystals. For MBBA (see table 2), measurements of T_1 [40, 41] and T_2 [41] have been reported for both isotropic and nematic phases. As an example, proton–spin decoupled spectra are shown in figure 8. The temperature dependence of T_1 and T_2 for aromatic and aliphatic carbons is illustrated in figure 9. The main feature is a large drop in T_2 when going from the isotropic to the nematic phase. The change in the temperature dependence of T_1 through the isotropic–nematic transition observed in these curves was not found in a previous study [40]. There is an apparent increase in T_1 on going from C_{15} to C_{18} (for the latter, T_1 has to be corrected to take into account the fact that it is for the CH_3 group and not for a CH_2 group), reflecting the increasing mobility along the *n*-butyl tail. Under the assumption of an anisotropic reorientation motion for the entire molecule, the diffusion constants and correlation times reported in table 4 are determined; $\tau_\parallel$ is found to be about 10^{-2} times shorter than $\tau_\perp$. Similar behaviour has recently been observed for measurements of T_1 on 5CB (see table 2) [42]; the same ratio between $\tau_\parallel$ and $\tau_\perp$ is observed, and $\tau_\perp$ at 56°C (isotropic phase) is found to be 10^{-9} s. However, no change in the temperature dependence of T_1 has been found on going from the isotropic to the nematic phase.

Table 4. Rotational constants of MBBA from ^{13}C N.M.R. [41].

T/K	$D_\perp$/cm^2 s^{-1}	$D_\parallel$/cm^2 s^{-1}	$\tau_\perp$/s	$\tau_\parallel$/s
302 (nematic)	$4{\cdot}4 \times 10^7$	$1{\cdot}1 \times 10^{10}$	$3{\cdot}8 \times 10^{-9}$	$1{\cdot}5 \times 10^{-11}$
353 (isotropic)	$2{\cdot}4 \times 10^8$	$5{\cdot}3 \times 10^{10}$	$6{\cdot}9 \times 10^{-10}$	$3{\cdot}1 \times 10^{-12}$

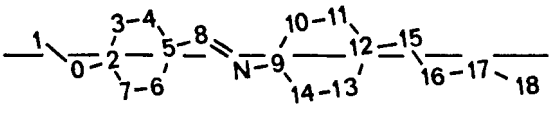

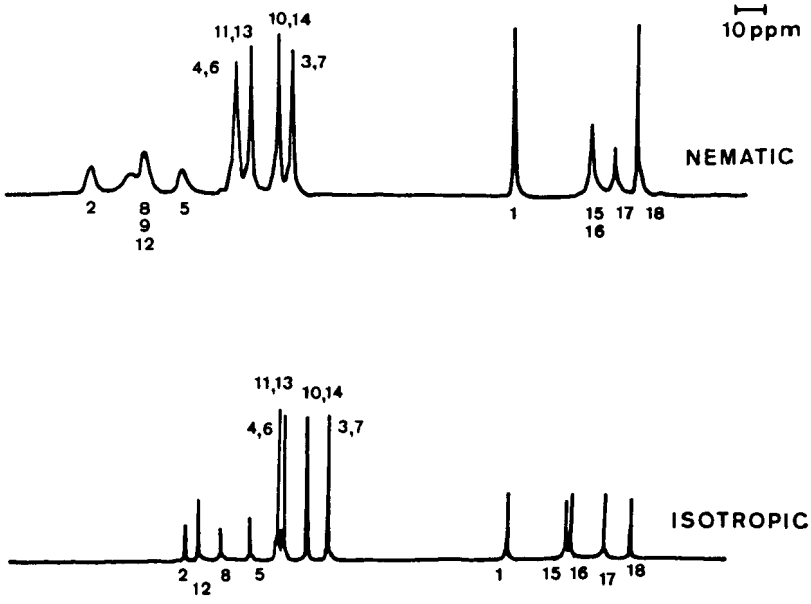

Figure 8. ^{13}C N.M R. spectra of MBBA. (After [41].)

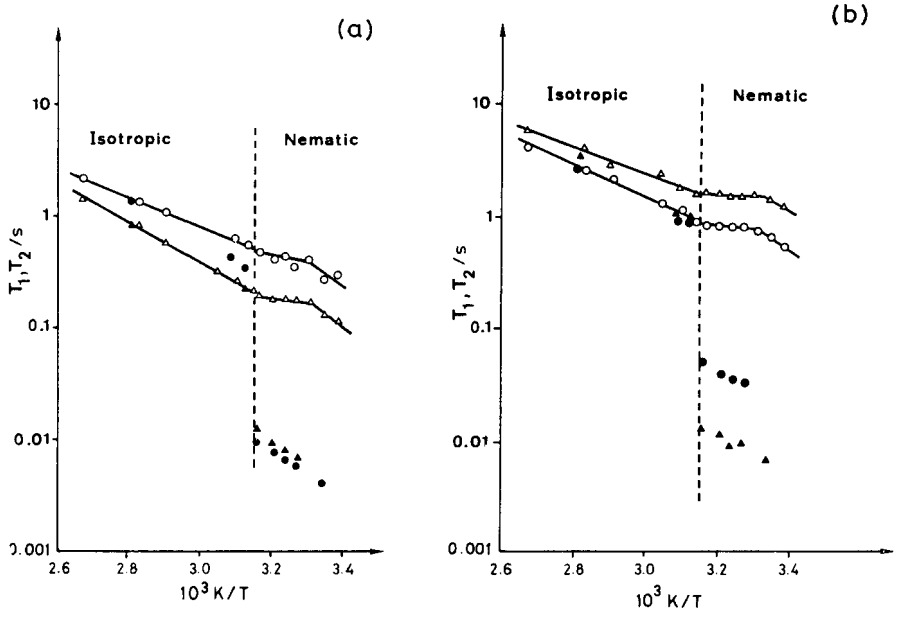

Figure 9. Relaxation times T_1 and T_2 for various carbon atoms in MBBA, as identified in figure 8: (*a*) ○, C_2, T_1; ●, C_2, T_2; △, C_3, C_7, T_1; ▲, C_3, C_7, T_2; (*b*) ○, C_1, T_1; ●, C_1, T_2; △, C_{15}, T_1; ▲, C_{15}, T_2. (After [41].)

The different behaviours observed for T_1 and T_2 show that the high-frequency motion is changed little by the isotropic–nematic transition, but that the low-frequency motion is considerably affected as a result of the completely different molecular constraints in the two phases.

4.3. ^2H *N.M.R.*

A few studies of the dynamics of liquid crystals have been performed using ^2H N.M.R. For MBBA, measurements of T_1 have been made on molecules deuteriated either on the phenyl rings [43, 44] or on the carbon atoms in the chain [45]. The spectrum of the phenyl deuterons in the nematic phase shows that four of the eight deuteron sites are inequivalent, indicating that the rings are rapidly rotating around their C_1–C_4 axes. The occurrence of four pairs of spectral lines is assigned [43] to small differences in C–C–D bond angles. Two sets of values are obtained for T_1, the temperature dependences of which are shown in figure 10. The deuterons with the shorter relaxation time are attributed to the aniline ring, while those with the longer relaxation time correspond to the benzylidene ring. There is no change in the average T_1 through the nematic–isotropic transition, and the apparent activation energy is about 35 kJ mol^{-1}. The data have been analysed by considering the O.D.F. mechanism, a fluctuation about the short axis or a reorientation around the para axes. It appears that the main relaxation mechanism is the latter (with different rates for the aniline and benzylidene rings); at 291 K this corresponds to an average correlation time τ_C of 9×10^{-10} s, in good agreement with dielectric relaxation measurements (§ 4.4). The O.D.F. contribution is found to be negligible, whereas the fluctuation about the short axis may add to T_1 to a slight extent. The study of the deuteriated aliphatic carbon atoms [45] leads to the temperature dependences of the various T_1 shown in figure 11. These results can be accounted for by considering molecular reorientations and internal motions only; the O.D.F. mechanism does not contribute. The mobility increases along the *n*-butyl tail, in agreement with the ^{13}C N.M.R. results (§4.2 and [41]). The methine deuteron has the slowest motion.

Measurements of T_1 on the methine deuteron of 4-*n*-pentyloxybenzylidene-4′-*n*-heptylaniline (50–7) in the I, N, S_A, S_C, S_B and S_H phases [46] have shown that there is a change in the temperature dependence at the N–S_A transition, but no change at

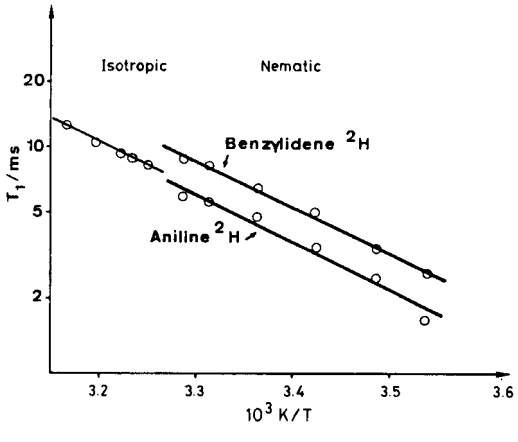

Figure 10. Temperature dependence of T_1 for the phenyl deuterons of MBBA. (After [43].)

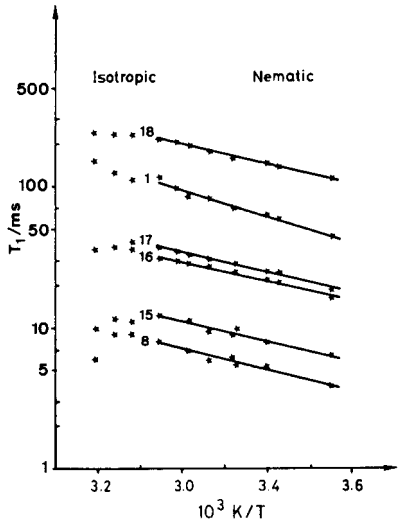

Figure 11. Logarithmic plot of T_1 versus $10^3/T$ for the deuterons in MBBA numbered as indicated in figure 8. Solid lines correspond to the data obtained in the nematic phase. (After [45].)

the various smectic–smectic transitions. The O.D.F. mechanism cannot account for these results, and so the main relaxation mechanism in the smectic phases is attributed to reorientation about the short molecular axis. The calculated correlation times range from 8×10^{-11} to 5×10^{-10} s, with an activation energy of 40 kJ mol^{-1}. These correlation times are much shorter than those determined from dielectric relaxation on 50–6 (figure 12).

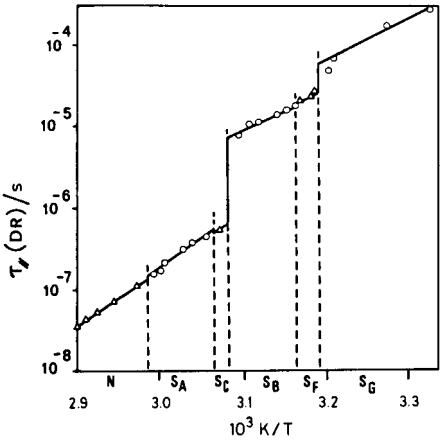

Figure 12. Dielectric relaxation time $\tau_{\parallel}$(DR) versus $10^3/T$ in the various mesophases of 50–6. (After [50].)

4.4. *Dielectric relaxation*

The 4-*n*-alkyl-4′-cyano biphenyl molecules (see table 2) constitute the simplest liquid crystal molecules for dielectric relaxation studies as there is only one polar group and the electric dipole moment lies approximately along the molecular long

axis. Dielectric measurements with the electric field parallel or perpendicular to the director have been performed on 7CB (see table 2) in the frequency range 10^5 to $2{\cdot}5 \times 10^8$ Hz [47]. From the quasi-static and high-frequency limiting permittivities, and by using the value of the order parameter determined by another technique, the correlation factor g can be deduced. The resulting values are $g_\parallel \approx 0{\cdot}30$ and $g_\perp \approx 0{\cdot}90$. The latter value indicates that perpendicular to the director the dipole components are oriented essentially at random, as a result of the small dipolar component in that direction.

In the isotropic phase a single relaxation is observed which corresponds to an isotropic motion (Debye type). In the nematic phase the parallel arrangement yields a single Debye-like relaxation, whereas perpendicular measurements show a broad $\varepsilon''_\perp$ absorption. The temperature dependence of the corresponding correlation times, τ(DR), is presented in figure 13. Note that $\tau_\parallel$(DR) corresponds to a rotational motion about an axis perpendicular to the director (motion about the molecular short axis), whereas in N.M.R. or E.S.R. such motion is characterized by a correlation time $\tau_\perp$.

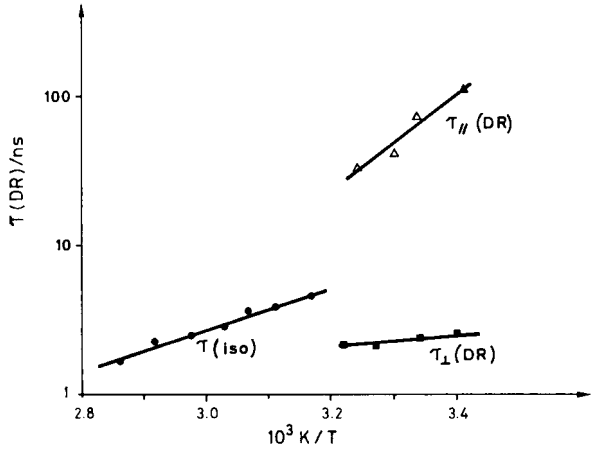

Figure 13. Dielectric relaxation times versus $10^3/T$ in the nematic phase ($\tau_\parallel$(DR) and $\tau_\perp$(DR)) and the isotropic phase (τ_{iso}). (After [47].)

In spite of the different autocorrelation functions in dielectric and magnetic relaxation, it is of interest to compare the order of magnitude of the correlation times derived by these techniques. The results shown in figure 13 for the isotropic phase are in fair agreement with the average correlation time ($\overline{\tau_R} = (\tau_\parallel \tau_\perp)^{1/2}$) obtained by ^{13}C N.M.R. on 5CB [42]. In the nematic phase the ratio $\tau_\parallel$(DR)/$\tau_\perp$(DR) ranges from 50 at 293 K to 15 at 308 K, which appears to be much smaller than found by N.M.R.

The treatment of dielectric relaxation in the nematic phase proposed in [25] has been successfully applied to these data. Furthermore, the relative intensities of the relaxation processes in the parallel and perpendicular measurements, estimated from the values at the maximum of $\varepsilon''_\parallel$ and $\varepsilon''_\perp$, agree satisfactorily with the theoretical prediction. It should be pointed out that the agreement is not so good with liquid crystal molecules which have internally rotatable polar groups.

Dielectric relaxation studies have also been performed on MBBA [48, 49]. For a sample oriented in a 1·2 T magnetic field, parallel measurements in the frequency range from 10^5 to 10^7 Hz [48] show a maximum in $\varepsilon''_\parallel$ at $1{\cdot}1 \times 10^6$ Hz at 295·7 K, and

agrees with a Debye-like relaxation. On the other hand, no relaxation is observed in this frequency range for perpendicular measurements. For a multi-domain sample investigations in the frequency range from 10^9 to 10^{10} Hz [49] show a relaxation in the nematic phase corresponding to correlation times from 2×10^{-10} to 6×10^{-10} s in the temperature range from 295 to 305 K. Comparison with the corresponding values obtained by ^{13}C N.M.R. and reported in table 4, shows that motions around the molecular short axis have a correlation time almost two orders of magnitude higher in dielectric relaxation, suggesting that in the latter case a cooperative motion could be involved (this interpretation is supported by the rotation correlation times τ_R obtained by ^1H N.M.R. and given in table 3). For motion around the molecular long axis, a smaller discrepancy is found.

The influence of the nature of the mesophase on the molecular dynamics investigated by dielectric relaxation is quite well illustrated by the studies performed on 50–6, 50–7, 50–8 and 60–6 [50–53]. The increase in dielectric anisotropy on passing through the sequence $I \rightarrow N \rightarrow S_A \rightarrow S_C \rightarrow S_B$ is shown in figure 14 for 50–7. The temperature dependence of $\tau_{\parallel}$ for 50–6 in the various mesophases is presented in figure 12. It is clear that there is no discontinuity at the N–S_A and S_A–S_C transitions, showing that, in spite of the layer structure of the smectic phases, the molecules are still able to rotate around their short axis. A significant slowing of the motion occurs at the S_A–S_B transition. However, even if the correlation time is one order of magnitude longer, there is still the possibility of the molecule rotating about its short axis.

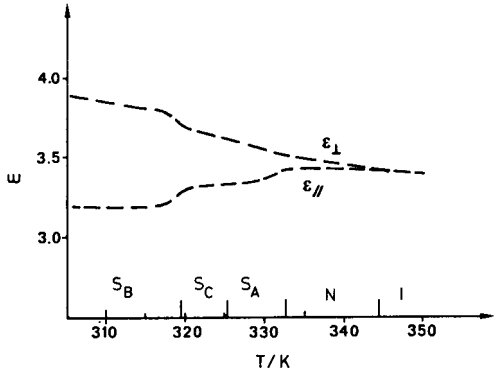

Figure 14. Temperature dependence of $\varepsilon_{\parallel}$ and $\varepsilon_{\perp}$ for 50–7. (After [51].)

4.5. *E.S.R.*

As an example of an E.S.R. investigation of molecular motion in liquid crystal mesophases, we will consider the studies performed on the various phases of 40–6 (see table 2) using nitroxide probes of different sizes and chemical structures. The structures of the probes are shown in table 1, and the principal magnetic axis system (x_1, y_1, z_1) for the nitroxide group is that given in figure 2. All the studies have been performed on single-domain samples. The transition temperatures for 40–6 are

$$K \xleftrightarrow{299\,K} S_B \xleftrightarrow{320{\cdot}3\,K} S_A \xleftrightarrow{327{\cdot}7\,K} N \xleftrightarrow{249{\cdot}9\,K} I$$

4.5.1. *P.D. Tempone Probe [54]*

The magnetic tensor for the probe molecule is not axially symmetric, and it appears that the y_1 axis is the most oriented along the magnetic field. The temperature dependences of the orientational order parameter $S_{y_1z_5}$ and the biaxiality $(S_{x_1y_5} - S_{z_1x_5})$ are shown in figure 15(*a*). Although the spectra can be accounted for by assuming an axially symmetric ordering potential, a better fit is obtained with a non-axially-symmetric potential defined by the two parameters $\lambda = \gamma_2/kT$ and $\varrho = \varepsilon/kT$. These two quantities are shown in figure 15(*b*).

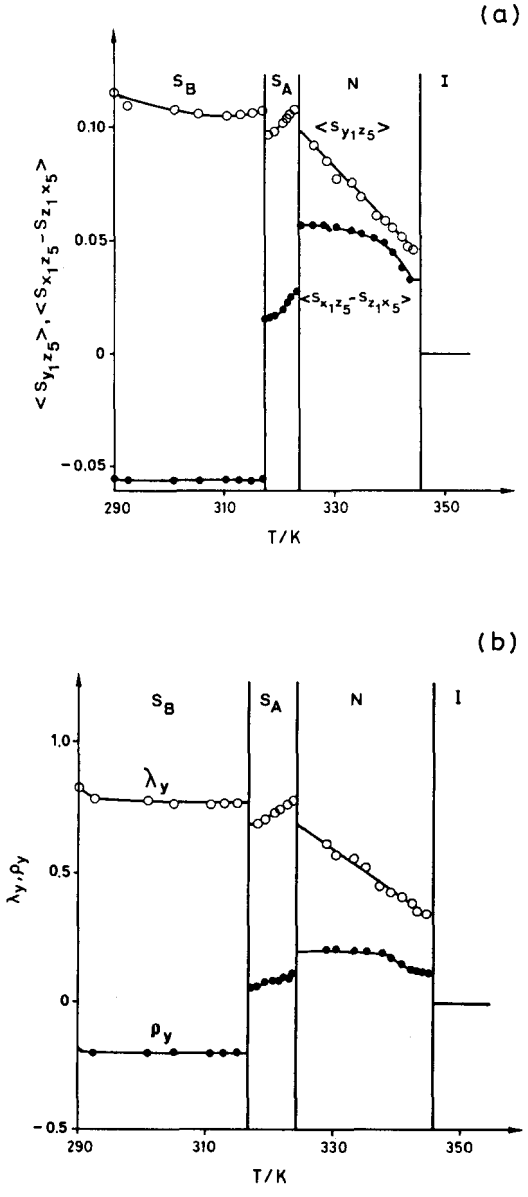

Figure 15. P.D. Tempone in 40–6. (*a*) Order parameter $S_{y_1z_5}$ and biaxiality $S_{x_1z_5} - S_{z_1x_5}$ versus temperature. (*b*) The parameters λ and ϱ of the ordering potential versus temperature. (After [54].)

As far as the dynamics are concerned, it should be noted that in the three mesophases the E.S.R. spectra of P.D. Tempone exhibit the features associated with motional narrowing. Such a result is not very surprising because of the small size of this probe. The mean correlation time, $\overline{\tau_R}$, is defined by the relation $\overline{\tau_R} = (6\overline{D_R})^{-1}$, with $\overline{D_R} = (D_\parallel D_\perp)^{1/2}$, $D_\parallel$ and $D_\perp$ being the parallel and perpendicular components of the rotational diffusion tensor. In figure 16 $\overline{\tau_R}$ is plotted against T^{-1} for the various mesophases. These results have been consistently interpreted by postulating that, as the temperature decreases, the P.D. Tempone is gradually transferred from the rigid core region of the 40–6 molecules to the more flexible and less ordered regions of the aliphatic tails as the system undergoes the successive transitions I → N → S_A → S_B. The similar apparent activation energies in the isotropic and nematic phases seem to indicate that the same type of motion occurs in these two phases, which is in agreement with the conclusions drawn from experiments with other spectroscopic techniques. The large decrease in $\overline{\tau_R}$ from S_A to S_B is surprising. It could correspond to a cavity-like arrangement of P.D. Tempone in the S_B phase, mainly in the aliphatic regions. There would be a partial freezing (or slowing down) of the hydrocarbon end-chains at the S_A → S_B transition such that the probe would be in a fairly well-defined cavity with a reduced frictional restriction to its motion, leading to a large decrease of $\overline{\tau_R}$. However, the residual end-chain motions would modulate the structure of the cavity, leading to a S.R.L.S. process contributing to the observed linewidths.

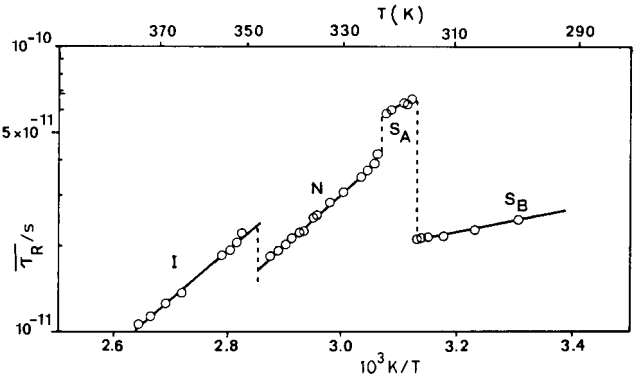

Figure 16. P.D. Tempone in 40–6; mean correlation time $\overline{\tau_R}$ versus $10^3/T$. (After [54].)

4.5.2. *P-Probe [55]*

In this probe molecule intramolecular motions may occur in such a way that the magnetic axes of the nitroxide group may be different from the rotational diffusion axes of the molecule. Furthermore, the mean conformation of the probe molecule may change with temperature and with the type of mesophase. Nevertheless, information about these behaviours can be derived from the values and the temperature dependence of the order parameters and the ordering potential coefficients. The correlation times $\overline{\tau_R}$ and $\tau_{R\perp}$ ($\tau_{R\perp} = (6D_\perp)^{-1}$) are plotted against T^{-1} in figure 17. In contrast to P.D. Tempone, it does not seem that any expulsion of the P-Probe occurs. In the isotropic phase the anisotropy parameter $N = D_\parallel/D_\perp$ is equal to 7, which suggests an almost completely extended molecule. The activation energy is the same as for P.D. Tempone, showing that the same molecular motions occur in both cases, in spite of the different molecular sizes. The isotropic–nematic transition does not

change the activation energy significantly, but there is a slowing of the motion about the short molecular axis. In the S_A phase the $\tau_{R\perp}$ values are still increased, but without any change in $\tau_{R\parallel}$. This indicates that there is no additional constraint upon motion about the molecular long axis of the probe, but the overall motion is slowed by the increase in frictional forces that results from a better packing in the S_A phase. It should be noted that in both nematic and smectic A phases the fit to the experimental spectra requires a contribution from the S.R.L.S. mechanism, the O.D.F. mechanism does not contribute in this frequency range. In the S_B phase, which is ordered within the layers, the observed discontinuity in $\overline{\tau_R}$ comes from a strong decrease in $\tau_{R\parallel}$, the rotational motion about the molecular long axis being constrained by the motional cooperativity required from the surrounding molecules.

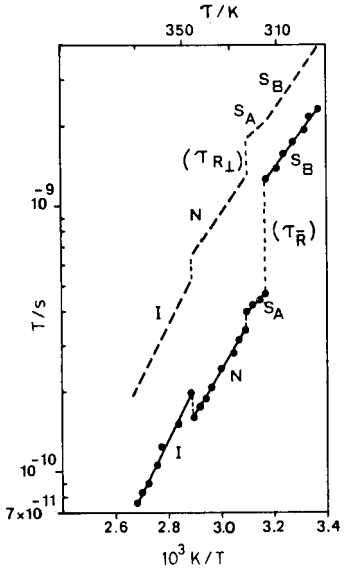

Figure 17. P-Probe in 40–6; $\overline{\tau_R}$ and $\tau_{R\perp}$ versus $10^3/T$. (After [55].)

4.5.3. *CSL Probe [56]*

In this probe the nitroxide group cannot undergo any intramolecular motion relative to the cholestane unit, and the intramolecular motions of the rather short aliphatic tail have little effect on the overall shape of the molecule. Thus, the CSL probe can be considered as a quasi-rigid probe with well-defined molecular axes, and the angles between the molecular long axis and the magnetic axes are known. The dynamics of the probe corresponds to the slow-motion regime, though the spectra show three well-resolved lines. The temperature dependences of $\overline{\tau_R}$ and $\tau_{R\perp}$ are shown in figure 18. In the nematic phase the observed anisotropy parameter ($N = 5$) is in agreement with the molecular geometry. The correlation times are in the range from 2×10^{-9} to 8×10^{-9} s, much longer than those of the other probes, which is to be expected because of the large size and high rigidity of the CSL probe. The order parameter is rather high; it is 0·77 at 51°C (the values found at the same temperature are 0·44 for the P-Probe and 0·10 for P.D. Tempone), and reaches 0·86 in the S_A and S_B phases. These high values reflect the fact that the CSL probe is very close to the

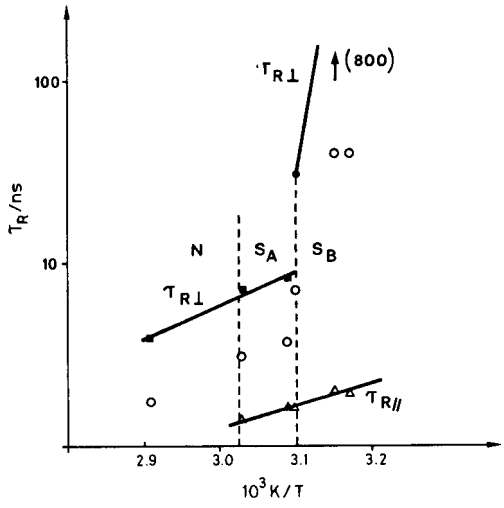

Figure 18. CSL in 40–6; correlation times versus $10^3/T$. △, $\tau_{R\parallel}$; ■, $\tau_{R\perp}$; ○, $\overline{\tau_R}$. (After [56].)

rigid core of the 40–6 molecules; there is no expulsion occurring at all. In the S_A and S_B phases the slowing of the parallel motion is comparable to that observed with the P-Probe, except that the CSL correlation time, $\tau_{R\parallel}$, is one order of magnitude longer. However, the perpendicular motion of the CSL probe in the S_A and S_B phases is considerably hindered (which is not observed with the other probes), and the correlation time $\tau_{R\perp}$ in the S_A phase is even outside the range of the E.S.R. technique. Under such conditions, the observation of E.S.R. spectra with well-resolved lines cannot be explained by considering only the dynamics of the individual probe. The proposed interpretation is that the CSL probe reorients itself in a local cage, the average and instantaneous conformations of which impose restrictions upon the motion of the probe, so that the overall dynamics are now determined by the combined effect of individual probe modes and collective modes of the surrounding molecules. The S.R.L.S. mechanism could be responsible for the dynamic cooperativity.

These results adequately illustrate the problems which result from the investigation of the molecular dynamics of liquid crystals by E.S.R. It is clearly shown that the requirement of an extrinsic probe, the motion of which is observed rather than the dynamics of the liquid crystal molecules, is the main problem. Indeed, the location of the probe is not known and can change with the type of mesophase. The best way to avoid this problem is to use an analogue of the liquid crystal molecule, bearing a nitroxide group, but this requires a specific synthesis. Another difficulty comes from the intramolecular motions of the probe. It can be avoided with the CSL probe, but this yields spectra from the slow-motion regime which are more difficult to analyse. However, the interest in the E.S.R. technique rests on the great sensitivity of the spectra to anisotropic dynamic behaviour and on the fact that this technique alone makes it possible to distinguish in the slow-motion regime the different types of motion (such as brownian diffusion or jumps).

5. Conclusions

The molecular dynamics of liquid crystals cover a very large frequency range, from intramolecular rotations to orientational order director fluctuations (collective elastic

fluctuations resulting from hydrodynamic effects). Among the spectroscopic techniques which can be used to investigate molecular motion, only ^{2}H N.M.R. and dielectric relaxation can, in principle, cover such a large frequency range. However, the studies which have been performed to date on liquid crystals have dealt mainly with high-frequency molecular motion (10^6–10^{12} Hz).

^{1}H N.M.R. provides information on the intermolecular contribution, whereas ^{13}C and ^{2}H N.M.R. allow us to investigate the motion of the different groups in the molecule. Dielectric relaxation leads to a fairly straightforward interpretation when the molecule has only one strong dipolar group lying along the molecular long axis, but in the other cases (when there are several dipolar groups, or the dipolar group is inclined to the molecular long axis) the analysis of the data on a molecular scale becomes very difficult. E.S.R. requires the use of a nitroxide probe, the location of which close to the rigid core or to the alkyl tails of the liquid crystal molecules makes it difficult to interpret the data.

The examples presented in this article show that, in order to interpret the molecular dynamics of liquid crystals, experiments have to be performed on very well aligned samples and by a variety of different spectroscopic techniques. Unfortunately, to date few systems have been investigated in this way.

References

[1] DEMUS, D., and RICHTER, L., 1978, *Textures of Liquid Crystals* (Verlag Chemie, Weinheim).

[2] GRAY, G. W., and GOODBY, J. W. G., 1984, *Smectic Liquid Crystals* (Leonard Hill).

[3] MAIER, W., and SAUPE, A., 1958, *Z. Naturf.* (*a*), **13**, 564; 1959, *Ibid.*, **14**, 882; 1960, *Ibid.*, **15**, 287.

[4] ABRAGAM, A., 1961, *The Principles of Nuclear Magnetism* (Oxford University Press).

[5] VISINTAINER, J. J., BOCK, E., DONG, R. Y., and TOMCHUK, E., 1975, *Can. J. Phys.*, **53**, 1483.

[6] LEWIS, J. S., TOMCHUK, E., and BOCK, E., 1983, *Molec. Crystals liq. Crystals*, **97**, 387.

[7] WEHRLI, F. W., and WIRTHLIN, T., 1976, *Interpretation of Carbon-13 N.M.R. Spectra* (Heyden).

[8] FARRAR, T. C., and BECKER, E. D., 1971, *Pulse and Fourier Transform N.M.R.* (Academic Press).

[9] MEHRING, M., 1976, *High Resolution N.M.R. Spectroscopy in Solids, Basic Principles and Progress NMR*, Vol. 11, edited by P. Diehl, E. Fluck and R. Kosfeld (Springer-Verlag), p. 112.

[10] PINES, A., and CHANG, J. J., 1974, *Phys. Rev.* A, **10**, 946.

[11] HAEBERLEN, U., 1976, *High Resolution N.M.R. Spectroscopy in Solids*, Suppl. 1 to Advances in Magnetic Resonance (Academic Press).

[12] SPIESS, H. W., 1983, *Colloid Polym. Sci.*, **261**, 193.

[13] SNIJDERS, J. G., DE LANGE, C. A., and BURNELL, E. G., 1983, *Israel J. Chem.*, **23**, 269.

[14] BECKMANN, P. A., EMSLEY, J. W., LUCKHURST, G. R., and TURNER, D. L., 1983, *Molec. Phys.*, **50**, 699.

[15] BERLINER, L. J. (editor), 1976, *Spin Labeling* (Academic Press).

[16] ATHERTON, N. M., 1973, *Electron Spin Resonance, Theory, Applications* (Wiley).

[17] GORDY, W., 1980, *Theory and Applications of Electron Spin Resonance* (Wiley).

[18] MONNERIE, L., 1982, *Static and Dynamic Properties of the Polymeric Solid State*, edited by R. A. Petrick and R. W. Richards (Reidel), p. 271.

[19] LUCKHURST, G. R., POUPKO, R., and ZANNONI, G., 1975, *Molec. Phys.*, **30**, 499.

[20] HILL, N., VAUGHAN, W. E., PRICE, A. H., and DAVIES, M., 1969, *Dielectric Properties and Molecular Behavior* (Van Nostrand).

[21] MCCRUM, N. G., READ, B. E., and WILLIAMS, G., 1967, *Anelastic and Dielectric Effects in Polymeric Solids* (Wiley).

[22] HEDVIG, P., 1977, *Dielectric Spectroscopy of Polymers* (Adam Hilger).

[23] WILLIAMS, G., 1979, *Adv. Polym. Sci.*, **33**, 59.
[24] DE JEU, W. H., 1978, *The Dielectric Permittivity of Liquid Crystals in Solid State Physics*, Suppl. 14, Liquid Crystals, edited by L. Liebert (Academic Press), p. 109.
[25] MEIER, G., and SAUPE, A., 1966, *Molec. Crystals liq. Crystals*, **1**, 515.
[26] BORDEWIJK, P., 1974, *Physica*, **75**, 146.
[27] WILLIAMS, W., COOK, M., and HAINS, P. J., 1972, *J. chem. Soc. Faraday Trans II*, **68**, 1045.
[28] FREED, J. H., 1977, *J. chem. Phys.*, **66**, 4183.
[29] NORDIO, P. L., and SEGRE, U., 1979, *The Molecular Physics of Liquid Crystals*, edited by G. R. Luckhurst and G. W. Gray (Academic Press), pp. 411, 427.
[30] NORDIO, P. L., and SEGRE, U., 1973, *Molec. Phys.*, **25**, 129.
[31] BECKMANN, P. A., EMSLEY, J. W., LUCKHURST, G. R., and TURNER, D. L., 1986, *Molec. Phys.*, **59**, 97.
[32] LUCKHURST, G. R., 1972, *Electron Spin Relaxation in Liquids*, edited by L. T. Muus and P. W. Atkins (Plenum Press), p. 411.
[33] POLNASZEK, C. F., BRUNO, G. U., and FREED, J. H., 1973, *J. chem. Phys.*, **58**, 3185.
[34] POLNASZEK, C. F., and FREED, J. H., 1975, *J. phys. Chem.*, **79**, 2283.
[35] DE GENNES, P. G., 1974, *The Physics of Liquid Crystals* (Clarendon Press).
[36] PINCUS, P., 1969, *Solid St. Commun.*, **7**, 415.
[37] GRAF, V., NOACK, F., and STOHRER, M., 1977, *Z. Naturf.* (*a*), **32**, 61.
[38] BLINC, R., VILFAN, M., LUZAR, M., SELIGER, J., and ZAGAR, V., 1978, *J. chem. Phys.*, **68**, 303.
[39] LEWIS, J. S., TOMCHUK, E., and BOCK, E., 1983, *Molec. Crystals liq. Crystals*, **97**, 387.
[40] HUTTON, M., BOCK, E., TOMCHUK, E., and DONG, R. Y., 1978, *J. chem. Phys.*, **68**, 940.
[41] OCHIAI, S., IIMURA, K., TAKEDA, M., OHUCHI, M., and MATSUSHITA, K., 1981, *Molec. Crystals liq. Crystals*, **78**, 227.
[42] LEWIS, J. S., TOMCHUK, E., HUTTON, H. M., and BOCK, E., 1983, *J. chem. Phys.*, **78**, 632.
[43] RUTAR, V., VILFAN, M., BLINC, R., and BOCK, E., 1978, *Molec. Phys.*, **35**, 721.
[44] VISINTAINER, J. J., DONG, R. Y., BOCK, E., TOMCHUK, E., BEWEY, D. B., KUO, A. L., and WADE, C. G., 1977, *J. chem. Phys.*, **66**, 3343.
[45] DONG, R. Y., LEWIS, J. S., TOMCHUK, E., and BOCK, E., 1978, *J. chem. Phys.*, **69**, 5314.
[46] DONG, R. Y., LEWIS, J. S., HAVELOCK, M. E., TOMCHUK, E., and BOCK, E., 1981, *J. magn. Reson.*, **45**, 223.
[47] DAVIES, M., MOUTRAN, R., PRICE, A. H., BEEVERS, M. S., and WILLIAMS, G., 1976, *J. chem. Soc. Faraday Trans. II*, **72**, 1447.
[48] RONDELEZ, F., and MIRREA-ROUSSEL, A., 1974, *Molec. Crystals liq. Crystals*, **28**, 173.
[49] MOSCICKI, J. K., NGUYEN, X. P., URBAN, S., WROBEL, S., RACHWALSI, M., and JANIK, J. A., 1977, *Molec. Crystals liq. Crystals*, **40**, 177.
[50] KRESSE, H., SELBMANN, CH., DEMUS, D., BUKA, A., and BATA, L., 1981, *Crystal. Res. Technol.*, **16**, 1439.
[51] BENGUIGUI, L., 1980, *J. Phys., Paris*, **41**, 341.
[52] BENGUIGUI, L., 1983, *Phys. Rev.* A, **28**, 1852.
[53] BENGUIGUI, L., 1984, *Phys. Rev.* A, **29**, 2968.
[54] LIN, W. J., and FREED, J. H., 1979, *J. phys. Chem.*, **83**, 379.
[55] MEIROVITCH, E., IGNER, D., IGNER, E., MORO, G., and FREED, J. H., 1982, *J. chem. Phys.*, **77**, 3915.
[56] MEIROVITCH, E., and FREED, J. H., 1980, *J. phys. Chem.*, **84**, 2459.